

Highly Linear Integrated Coherent Receivers for Microwave Photonic Links

Jonathan Klamkin¹, Leif A. Johansson², Anand Ramaswamy², Nobuhiro Nunoya²,
Sasa Ristic², Uppili Krishnamachari², Janet Chen², John E. Bowers², Steven P.
DenBaars^{1,2}, Larry A. Coldren^{1,2}

¹Materials Department, University of California, Santa Barbara, CA 93106

²Electrical and Computer Engineering Department, University of California, Santa Barbara, CA 93106

Email: klamkin@engineering.ucsb.edu

Abstract: A coherent receiver with feedback was developed to linearly demodulate the phase of an analog signal. The receiver demonstrates a spur-free dynamic range of $125 \text{ dB}\cdot\text{Hz}^{2/3}$ at a signal frequency of 300 MHz.

©2009 Optical Society of America

OCIS codes: (250.5300) Photonic Integrated Circuits; (250.3140) Integrated Optoelectronic Devices

1. Introduction

Phase modulation can be used to improve the signal-to-noise ratio (SNR) and spur-free dynamic range (SFDR) of microwave photonic links because phase modulation is not limited in input modulation swing and is inherently linear using certain electro-optic devices [1]. To overcome the inherent nonlinearity of a traditional interferometer-based phase demodulator, a balanced receiver with feedback to a reference tracking phase modulator was developed (Fig. 1). The feedback reduces the phase difference between the signal and local oscillator. This effectively reduces the signal swing of the demodulator thereby suppressing the interferometer nonlinearities and leading to an improvement in SFDR. Balanced detection has several advantages such as the ability to suppress common mode relative intensity noise of the laser source as well as amplifier noise. Additionally, considering that most 2x1 combiners inherently exhibit a loss of 3 dB, a higher SNR can be achieved with balanced detection because the detected signal power is increased. Additionally, push pull drive to symmetric tracking phase modulators can be used to overcome the nonlinear characteristics of the integrated tracking phase modulator. For stable operation at high frequency the delay of the feedback loop must be kept short, therefore a monolithic approach is required to realize a compact receiver architecture. A similar feedback approach was demonstrated in [2] whereby an attenuation-counter-propagating phase modulator was employed, which is free of propagation delay.

The monolithic photonic integrated circuit (PIC) developed here consists of a high power balanced uni-traveling-carrier photodiode (UTC-PD), a compact 2x2 multimode interference (MMI) coupler, and multi-quantum well reference phase modulators. This PIC is hybrid integrated with an electronic integrated circuit (EIC) that provides transconductance amplification of the feedback signal for increased loop gain.

2. Device Design

For the integrated UTC-PDs, novel concepts such as absorption profile modification, charge compensation, and partially depleted absorption were incorporated to realize high saturation current and high linearity [3]. PD A

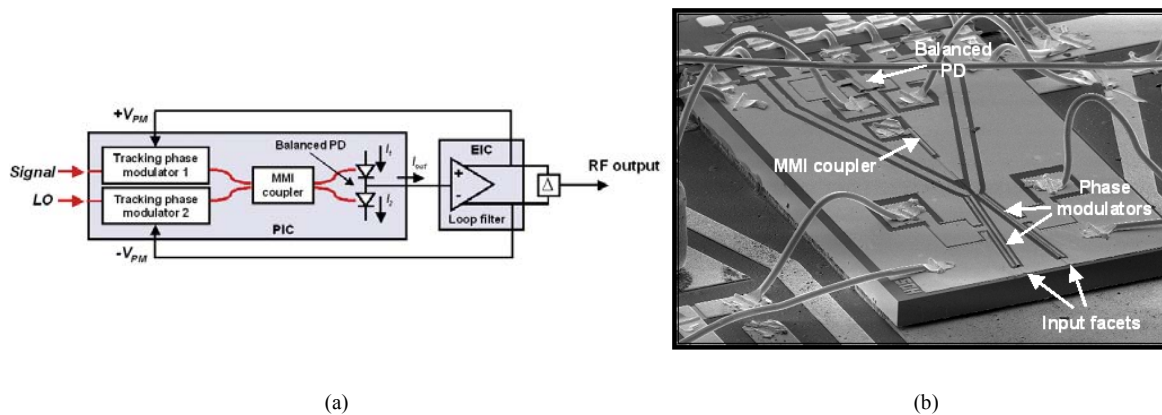


Figure 1. (a) Schematic of coherent integrated receiver with feedback and push-pull drive to tracking phase modulators. (b) Plan view SEM image of a PIC mounted on a carrier with an EIC (EIC out of view).

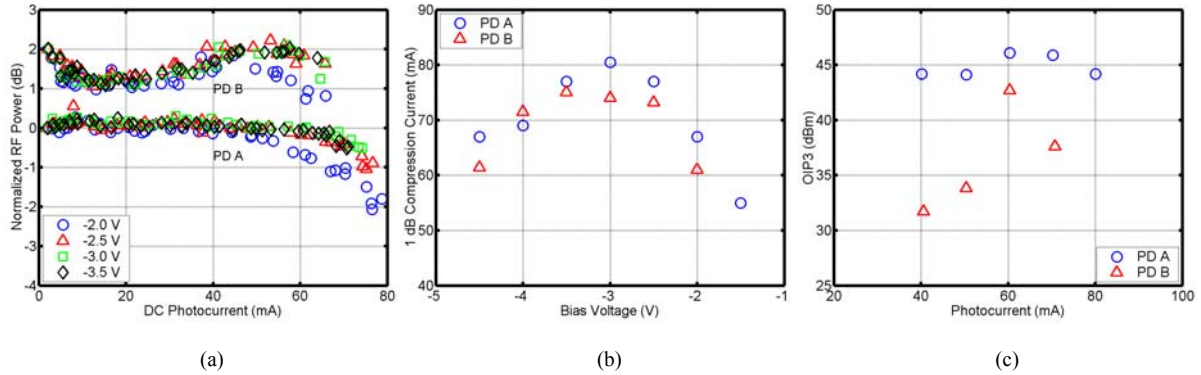


Figure 2. (a) Normalized RF power as a function of DC photocurrent at 1 GHz. The data for PD A is normalized to 0 dB and that for PD B to 2 dB. (b) 1-dB compression current as a function of bias voltage. (c) Two-tone OIP3 as a function of photocurrent.

incorporated a low overlap of the optical mode with the absorber layer resulting in a long absorption profile and low front-end saturation. PD B incorporated a collector doping of $3E16 \text{ cm}^{-3}$ and a low and graded absorber doping. Both general interference surface ridge (SR) MMI couplers and restricted interference deep ridge (DR) MMI couplers were explored, the latter for reducing the loop delay. Current injection tuning was incorporated into the

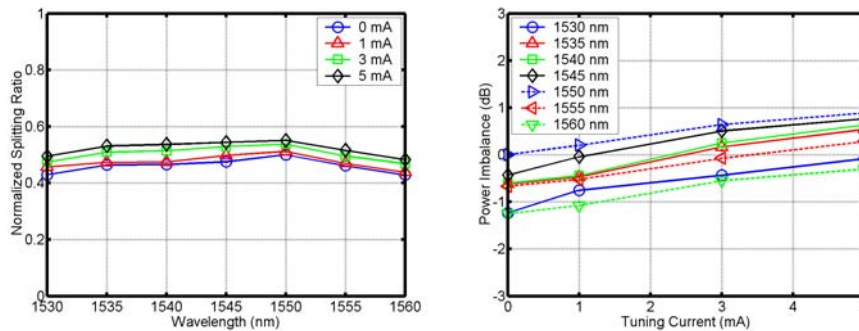


Figure 3. (a) Normalized splitting ratio as a function of input wavelength for various tuning currents. (b) Power imbalance as a function of tuning current for various wavelengths.

MMI couplers for fine tuning the output power splitting ratio [4]. The quantum well (QW) design of the reference phase modulators was optimized for realizing low V_π , low insertion loss, low absorption modulation, and improved linearity. Modulator A consisted of 28 compressively strained QWs, and 29 tensile strained barriers. The QW width was 50 Å, and the barrier width was 70 Å. The difference in energy between the QW and barrier in the conduction band was 97.3 meV. Modulator B contained 22 compressively strained QWs, and 23 tensile strained barriers. The QW width was 100 Å, the barrier width was 50 Å, and the conduction band energy difference was 69.6 meV. The PICs also incorporated quantum well intermixing (QWI) to shift the band edge of the QWs in the passive regions post growth to eliminate the tradeoff between phase modulation efficiency and passive loss.

3. Results and Discussion

Figure 2 shows the measurement results for the PDs. The peak 1 dB compression current for PD A and PD B was 80.5 mA and 75 mA respectively. The two-tone OIP3 for these PDs at 60 mA was 46.1 dBm and 42.7 dBm respectively. PD A was also measured at 80 mA and demonstrated an OIP3 of 44.2 dBm. The tuning properties of the SR MMI couplers were also characterized (Fig. 3). The output power splitting could be fine tuned to 3-dB splitting over a broad wavelength range with low levels of injected current. The efficiency, loss, and phase change were measured for the phase modulators (Fig. 4). The $V_\pi \cdot L$ of modulator A was 1.52 V·mm and that of modulator B was 1.29 V·mm. The loss incurred between 0 V and V_π and the insertion loss was 1.2 dB and 1.03 dB for modulator A, and 7.0 dB and 1.8 dB for modulator B. The ratio of the linear to cubic coefficient (A_1/A_3) was 19.5 for modulator A and 36.5 for modulator B.

OMK4.pdf

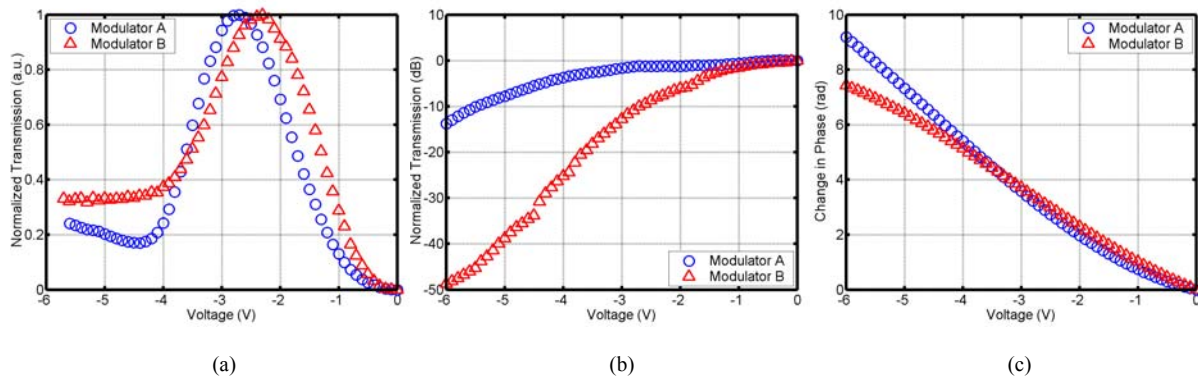


Figure 4. (a) Normalized MZM transmission, (b) normalized EAM transmission, and (c) phase change as a function of bias voltage.

The PIC and EIC were hybrid integrated on a common ceramic carrier. The chips were electrically connected with a series of wirebonds, which transport the differential output signal of the balanced PD from the PIC to the EIC, and the tracking phase modulator drive signal from the EIC to the PIC. Figure 5 shows the experimental setup used to characterize the integrated receivers and the results of SFDR measurements. Using the SR coherent receiver in a link experiment, the demonstrated SFDR for signal frequencies of 300 MHz, 500 MHz, and 1 GHz was $125 \text{ dB}\cdot\text{Hz}^{2/3}$, $121 \text{ dB}\cdot\text{Hz}^{2/3}$, and $113 \text{ dB}\cdot\text{Hz}^{2/3}$ respectively. Using a DR coherent receiver with QWI for low passive loss, and efficient phase modulators, the projected SFDR was improved by 6 dB.

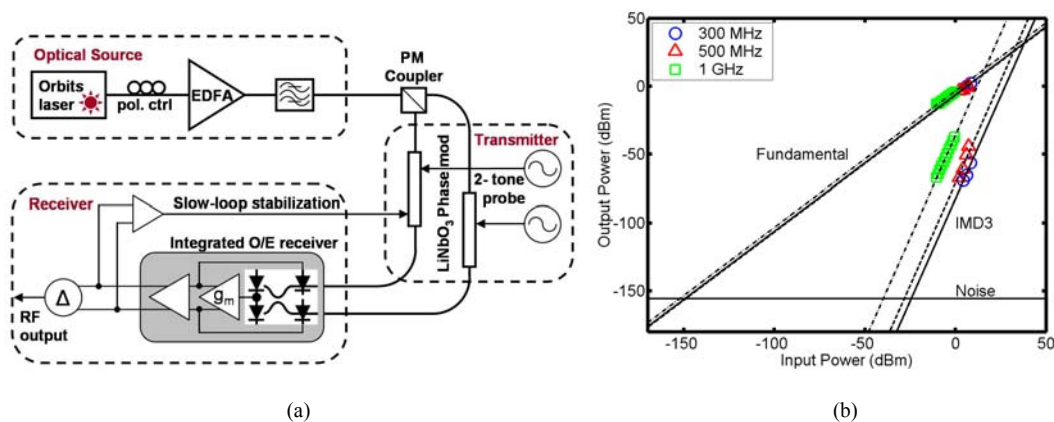


Figure 5. (a) Analog link experimental test setup. (b) SFDR measurements for different input signal frequencies.

4. Conclusions

A novel coherent receiver with feedback was developed to suppress the nonlinearities of an interferometer-based phase demodulator so that the advantages of phase modulation could be realized. When used in a link experiment, this receiver demonstrated up to a 14 dB improvement in SFDR compared to open loop operation (no feedback).

5. Acknowledgement

The authors acknowledge Northrop Grumman Space Technology for providing the EIC. This work was supported by the DARPA PHOR-FRONT program under USAF contract FA8750-05-C-0265.

6. References

- [1] L. A. Johansson, et al., *International Microwave Symposium (IMS)*, 2007.
- [2] Y. Li, P. R. Herczfeld, *Journal of Lightwave Technology*, vol. 24, pp. 3709-3718, 2006.
- [3] J. Klamkin, et al., *Device Research Conference (DRC)*, 2008.
- [4] J. Leuthold and C. H. Joyner, *Journal of Lightwave Technology (JLT)*, vol. 19, pp. 700-707, 2001.